

Phase-stepping interferometry of GaAs nanowires: Determining nano-wire radius

D. J. Little, R. L. Kuruwita, A. Joyce, Q. Gao, T. Burgess, C. Jagadish, and D. M. Kane

Citation: [Applied Physics Letters](#) **103**, 161107 (2013); doi: 10.1063/1.4825153

View online: <http://dx.doi.org/10.1063/1.4825153>

View Table of Contents: <http://scitation.aip.org/content/aip/journal/apl/103/16?ver=pdfcov>

Published by the [AIP Publishing](#)



Re-register for Table of Content Alerts

Create a profile.



Sign up today!



Phase-stepping interferometry of GaAs nanowires: Determining nano-wire radius

D. J. Little,^{1,a)} R. L. Kuruwita,¹ A. Joyce,¹ Q. Gao,² T. Burgess,² C. Jagadish,² and D. M. Kane¹

¹*MQ Photonics Research Centre, Department of Physics and Astronomy, Macquarie University, North Ryde, Sydney, NSW 2109, Australia*

²*Department of Electronic Materials Engineering, Research School of Physics and Engineering, Australian National University, Canberra, ACT 0200, Australia*

(Received 9 July 2013; accepted 30 September 2013; published online 15 October 2013)

Phase stepping interferometry is used to measure the size of near-cylindrical nanowires. Nanowires with nominal radii of 25 nm and 50 nm were used to test this by comparing specific measured optical phase profile values with theoretical values calculated using a wave-optic model of the Phase stepping interferometry (PSI) system. Agreement within 10% was found, which enabled nanowire radii to be predicted within 4% of the nominal value. This demonstration highlights the potential capability for phase stepping interferometry to characterize single nanoparticles of known geometry in the optical far-field. © 2013 AIP Publishing LLC. [<http://dx.doi.org/10.1063/1.4825153>]

Phase stepping interferometry (PSI) is an interferometric microscopy technique used to measure 3D surface height profiles with sub-nanometre accuracy.^{1,2} Although the use of PSI is reasonably widespread, quantitative 3D metrology is limited by a number of measurement artifacts, including diffraction-related artifacts that occur due to the use of conventional, far-field optics. An example of this are the so-called “batwing” artifacts commonly observed when looking at step-height profiles.^{3,4} Several wave-optic based models have been proposed which can correct for certain diffraction-related artifacts.^{5,6}

We have previously proposed a scheme whereby the size of nanoparticles of a known geometry can be determined using PSI by modelling and correcting for diffraction-related artifacts.⁷ Here, we present an experimental proof-of-principle of this technique by measuring the radius of GaAs nanowires. Nanowires were fabricated using metal organic chemical vapour deposition to be around 2–3 μm in length,^{8,9} before being transferred to the flat silicon surface via mechanical rubbing. Once transferred, nanowires lay prone on the silicon surface. Two batches of nanowires were studied, consisting of nanowires with nominal radii of 25 nm and 50 nm, with a standard deviation of 9% and 7%, respectively, measured using FESEM.

The instrument used to study the nanowires was a Bruker-AXS NT-9800 optical surface profiler, with a 0.80 numerical aperture, 115 \times Mirau objective, and possessing an adjustable collar so that the peak fringe contrast can be aligned with the focal plane of the objective. PSI was used to obtain the optical phase profile at the image plane of the instrument.¹⁰ The X- and Y-axes of the NT-9800 were calibrated using a 20 μm pitch grating. Uncertainty of measurements in X and Y was $\pm 2.5\%$. The Z-axis of the NT-9800 was calibrated using a reference laser. Phase (Z-axis) measurements have an uncertainty of 2.5 mrad. Optical phase profiles were averaged over 64 measurements (the

maximum permitted by the NT-9800 software) to minimize random noise. An example of a measured phase profile is shown in Fig. 1, which readily exhibits diffraction-related artifacts; notably a width of 400 nm compared to the ~ 25 nm nanowire radius, and a maximum optical phase of 0.178 rad; just 15% of the value that would be expected under a ray-optic approximation. Optical phase profiles of the nanowires were characterized by measuring the 1/e width of the phase profile, denoted w_ϕ and the optical phase along the nanowire axis, denoted ϕ_p .

Statistics of measured widths w_ϕ and ϕ_p are shown in Table I. Measured w_ϕ are very close to the 400 nm for both batches of nanowires, indicating that the 115 \times Mirau objective used in this study is well approximated by an aberration-free objective with a numerical aperture of 0.8. Uncertainties in the mean values were calculated by dividing the standard deviation by the square root of the sample size. Next, ϕ_p is theoretically modelled as a function of nanowire radius to compare how well it corresponds to the measured values.

The height profile of the nanowires is approximated as an infinite circular cylinder of radius, R , centered and oriented along the y -axis, is expressed as

$$z(x, y) - z_{\text{ref}} = \begin{cases} R + \sqrt{R^2 - x^2} & |x| \leq R \\ 0 & |x| > R, \end{cases} \quad (1)$$

where z_{ref} is an arbitrary reference height. In the theoretical formulation, the optical phase profile at the image plane is found using the following PSI equation:⁷

$$\phi_{\text{image}}(x, y) - \phi_{\text{ref}} = \tan^{-1} \left(\frac{\sin(2k(z(x, y) - z_{\text{ref}})) * \tau(x, y)}{\cos(2k(z(x, y) - z_{\text{ref}})) * \tau(x, y)} \right), \quad (2)$$

where $\tau(x, y)$ is the impulse response of the OSPs imaging system and * denotes convolution. The impulse response of the imaging system of the OSP, $\tau_{\text{OSP}}(x, y)$ can be approximated as

^{a)}Author to whom correspondence should be addressed. Electronic mail: douglas.little@mq.edu.au

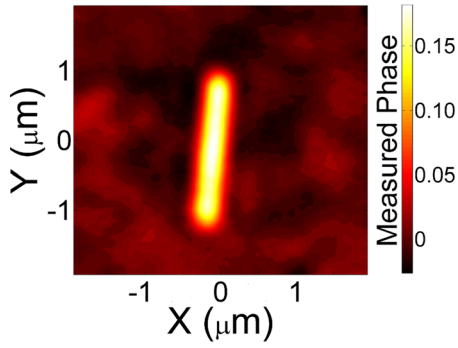


FIG. 1. Optical phase profile measured using PSI of a coherent wave ($\lambda = 514$ nm) reflected from a ~ 25 nm radius GaAs nanowire on a silicon substrate.

$$\tau_{\text{OSP}}(x, y) = J_1(\text{NA} \times k\sqrt{x^2 + y^2})/\sqrt{x^2 + y^2}. \quad (3)$$

A plot of ϕ_p calculated using Eq. (2) is shown in Fig. 2 (grey curve). This curve shows ϕ_p increasing monotonically with R until a value of around 70 nm. Here, there is a transition from positive to negative ϕ_p , with a second monotonically increasing region following this transition region.

The individual measured values of ϕ_p at $R = 25$ nm and 50 nm are also plotted in Fig. 2. It can be seen that there is a systematic discrepancy between the calculated and measured values of ϕ_p for both sets of nanowires. This discrepancy arises because the effect of geometric shadowing, depicted in Fig. 3, needs to be corrected for. Geometric shadowing manifests as a position-dependent modification of the impulse response. This removes the shift-invariance of the optical system and so Eq. (2) becomes

$$\phi_{\text{image}}(x, y) - \phi_{\text{ref}} = \tan^{-1} \left(\frac{\iint \sin(2k(z(x', y') - z_{\text{ref}}))\tau(x, x', y, y')dx'dy'}{\iint \cos(2k(z(x', y') - z_{\text{ref}}))\tau(x, x', y, y')dx'dy'} \right). \quad (4)$$

The most significant effect of geometric shadowing is the reduced amount of light collected by the objective from points near the nanowire. To model this, $\tau(x, x', y, y')$ is approximated as

$$\tau(x, x', y, y') = (1 - \sigma(x'))\tau_{\text{OSP}}(x - x', y - y'), \quad (5)$$

where σ is the fraction of the solid angle blocked by the nanowire that would otherwise be collected by the objective.

TABLE I. Statistical summary of measured w_ϕ and ϕ_p .

Quantity	Nanowire radius (nominal) (nm)	Sample size	Mean	Standard deviation
w_ϕ	50	17	404 nm \pm 4.0 nm	18 nm (4.5%)
w_ϕ	25	13	411 nm \pm 8.0 nm	29 nm (7.1%)
ϕ_p	50	17	0.721 rad \pm 0.034 rad	0.141 rad (19.6%)
ϕ_p	25	13	0.198 rad \pm 0.008 rad	0.030 rad (15.2%)

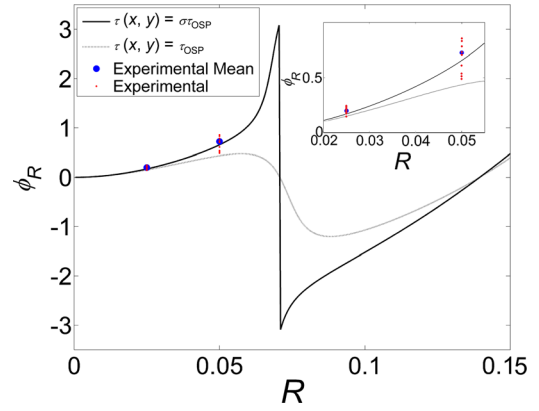


FIG. 2. ϕ_p calculated as a function of R using $\tau = \sigma\tau_{\text{OSP}}$ (corrected for geometric shadowing—black curve) and $\tau = \tau_{\text{OSP}}$ (not corrected for geometric shadowing—light curve). Experimental data are denoted by small red circles, experimental means are denoted by large blue circles. Inset: Expansion of the region from $R = 0.20$ to 0.55. Reprinted with permission from Little *et al.*, European Conference on Lasers and Electro-Optics, Munich, Germany, 12–16 May 2013, Paper No. PD-B.9. Copyright 2013 IEEE.

For the cylindrical height profile expressed in Eq. (1), σ is calculated to be¹¹

$$\sigma(x) = \pi^{-1} \cos^{-1}(\alpha/\beta) - \pi^{-1}(\alpha/\beta)\sqrt{1 - (\alpha/\beta)^2}, \quad R \leq |x| \leq R(1 + \gamma)/(1 - \gamma), \quad (6)$$

where $\alpha = \pi/2 - 2\tan^{-1}(R/x)$, $\beta = \sin^{-1}(\text{NA})$, and $\gamma = \tan(0.5\sin^{-1}(\text{NA}))$. It can be seen by inspection of Eq. (6) that σ increases monotonically from 0.5 to 1 over the applicable domain (R to $3R$ for a numerical aperture of 0.8).

A plot of ϕ_p corrected for geometric shadowing, calculated using Eqs. (4) and (5) is shown in Fig. 2 (black curve). The calculated value of ϕ_p at $R = 25$ nm and 50 nm was found to be 0.174 and 0.659, respectively, a difference of 0.024 ± 0.008 and 0.062 ± 0.034 , respectively, from the measured mean of ϕ_p . Using the measured mean of ϕ_p yields predicted nanowire radii of 26 nm and 52 nm for the two nanowire batches, which is accurate to within 4% of the nominal values of 25 nm and 50 nm. This result demonstrates phase stepping interferometry has great potential for application to measuring the size of nanoparticles of known geometry. The precision to which the radius of a single nanowire can be predicted is estimated from the measured standard deviation of ϕ_p to be around 5 nm and 7 nm for nanowires with nominal radii of 25 nm and 50 nm, respectively. The

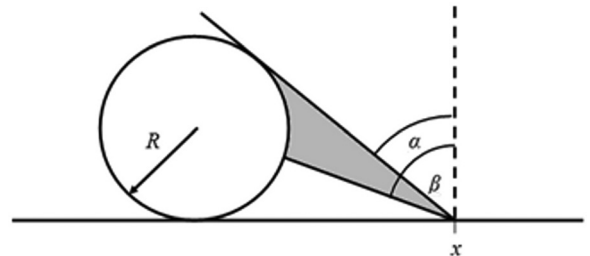


FIG. 3. Diagram showing how part of the solid angle light is scattered from x is blocked by the nanowire (grey area), resulting in a reduction of the impulse response at that point.

standard deviation in nanowire radii measured using electron microscopy was 9% for the 25 nm radius nanowires and 7% for the 50 nm radius nanowires, so approximately 50% of the observed standard deviation in ϕ_p can be attributed to variability in the size of the nanowires themselves.

To test the calculated ϕ_p across a continuous range of values of R , tapered nanowires were fabricated and studied. A scanning electron microscope image is shown in Fig. 4(a), showing a tapered nanowire to consist of two roughly linear taper sections; one with the radii varying from 160 nm to 60 nm over a length of 3.35 μm and a second with radii varying from 50 nm to 30 nm over a length of 0.56 μm , with an

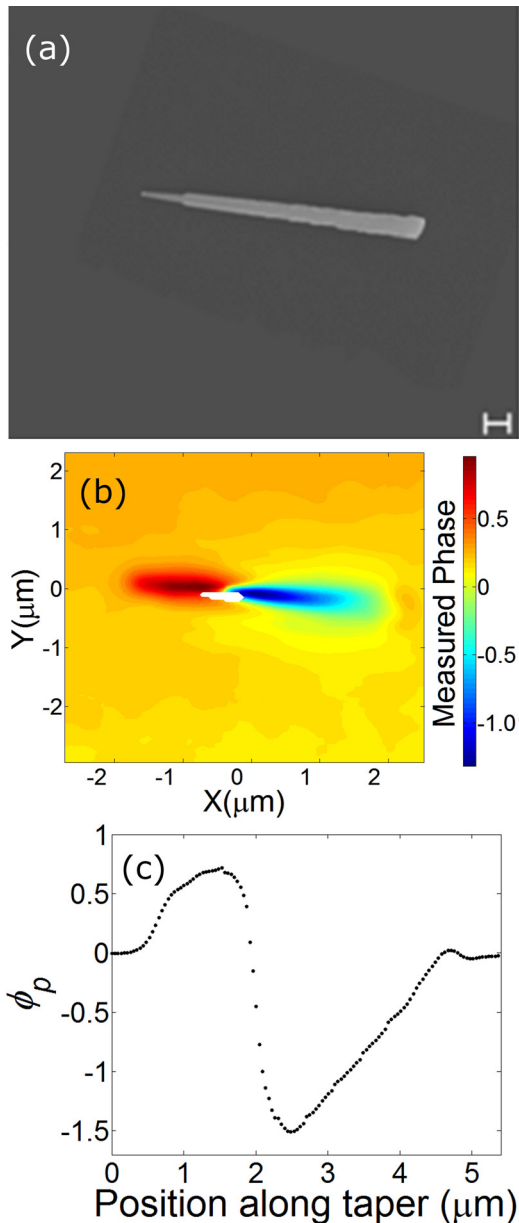


FIG. 4. (a) Scanning electron micrograph of a tapered nanowire. The scale bar is 1 μm in length. The original image has been rotated and filled to match the scale and orientation of the optical phase profile. (b) Optical phase profile measured using PSI of a coherent wave ($\lambda = 514 \text{ nm}$) reflected from the same tapered nanowire. White regions represent points where the Bruker-AXS NT-9800 OSP was unable to make a PSI measurement. (c) Peak phase as a function of position along the taper, starting at the narrow end. Reprinted with permission from Little *et al.*, European Conference on Lasers and Electro-Optics, Munich, Germany, 12–16 May 2013, Paper No. PD-B.9. Copyright 2013 IEEE.

uncertainty of $\pm 5 \text{ nm}$ for all quoted values. Fig. 4(b) shows the corresponding optical phase profile measured using PSI. The sharp transition from positive to negative ϕ_p , a key feature in the calculated ϕ_p vs R curve, is clearly evident, further verifying the accuracy of the theoretical model. The measured ϕ_p does not vary between the same extremes as the calculated ϕ_p vs R curve. This is a consequence of using tapered nanowires, where the theory is for uniform nanowires of effectively infinite length.

This proof-of-principle demonstration highlights the potential for PSI to be used for nanometrology on objects of known geometry. The advantages to being able to perform nanometrology using PSI, and in the optical far-field, in general, are quite profound. Optical measurement benefits from being able to penetrate through transparent media; and it is far more conducive to rapid, automated measurement compared to conventional nanometrology techniques (such as electron- and atomic-force-microscopy). In addition, it can be naturally adapted into conventional optical systems, potentially enabling its use in conjunction with other optical characterization techniques.

There are several caveats to using this technique, however; the most important of which is the requirement to know the sample geometry in advance. The success of this technique also depends on how well the sample geometry conforms to the ideal surface used in the model. The presence of surface roughness, for example, will detract from the precision of this technique (depending on the power spectrum of the surface noise). Nanoparticles must also be sufficiently dispersed, as nanoparticles that are too close together will affect the measurement of each. This can potentially be accounted for in the model by parameterizing the surface as a double-particle. Finally, there is a requirement to accurately characterize the impulse response (or equivalently, the optical transfer function of the PSI system). The impulse response can be estimated based on the known aberrations in the optical system, by decomposing the optical transfer function into a series of Zernike polynomials. The impulse response in Eq. (3) arises from approximating the optical transfer function as the lowest-order Zernike polynomial (i.e., a constant). Improvements in accuracy may be possible with the addition of more Zernike polynomials in the optical transfer function. Alternatively, there are schemes for measuring the impulse response directly.^{12–14}

In conclusion, we have demonstrated that PSI can be used to measure the radius of cylindrical nanowires with nominal radii of 25 nm and 50 nm to within 4% of their nominal value. This relies on calibration of the experimental optical phase measurements to the results of a theoretical wave-optic model of the imaging of the nanowire by the PSI, modified to account for geometric shadowing due to the nanowire. Future refinements of the theoretical model may yield further improvements in measurement accuracy. The precision of this technique was estimated to be 5–7 nm based on the standard deviation of the experimental measurements, with about half of this variability attributable to variability in the size of the nanowires themselves. This proof-of-principle study opens up the prospect of characterising single nanoparticles in the optical far-field using existing PSI instrumentation.

This research was supported by Australian Research Council Grant Nos. LE110100024 and DP130102674, a Macquarie University Research Development Grant, and the Australian National Fabrication Facility (ANFF).

- ¹B. Bhushan, J. C. Wyant, and C. L. Koliopoulos, *Appl. Opt.* **24**, 1489 (1985).
- ²B. S. Lee and T. C. Strand, *Appl. Opt.* **29**, 3784–3788 (1990).
- ³A. Harasaki and J. C. Wyant, *Appl. Opt.* **39**, 2101 (2000).
- ⁴F. Gao, R. K. Leach, J. Petzing, and J. M. Coupland, *Meas. Sci. Technol.* **19**, 015303 (2008).
- ⁵A. Krywonos, J. E. Harvey, and N. Choi, *J. Opt. Soc. Am. A* **28**, 1121–1138 (2011).
- ⁶J. M. Coupland and J. Lobera, *Meas. Sci. Technol.* **19**, 074012 (2008).
- ⁷D. J. Little and D. M. Kane, *Opt. Express* **21**, 15664–15672 (2013).
- ⁸J. Zou, M. Paladugu, H. Wang, G. J. Auchterlonie, Y.-N. Guo, Y. Kim, Q. Gao, H. J. Joyce, H. H. Tan, and C. Jagadish, *Small* **3**, 389 (2007).
- ⁹H. J. Joyce, Q. Gao, H. H. Tan, C. Jagadish, Y. Kim, X. Zhang, Y. Guo, and J. Zou, *Nano Lett.* **7**, 921 (2007).
- ¹⁰P. Hariharan, B. F. Oreb, and T. Eiju, *Appl. Opt.* **26**, 2504 (1987).
- ¹¹D. J. Little, R. L. Kuruwita, A. Joyce, Q. Gao, T. Burgess, C. Jagadish, and D. M. Kane, “Nanoparticle measurement in the optical far-field,” in *European Conference on Lasers and Electro-Optics, Munich, Germany, 12–16 May 2013*, Paper No. PD-B.9.
- ¹²M. R. Foreman, C. L. Giusca, J. M. Coupland, P. Török, and R. K. Leach, *Meas. Sci. Technol.* **24**, 052001 (2013).
- ¹³Y. Cotte, F. M. Toy, C. Arfire, S. S. Kou, D. Boss, I. Bergoënd, and C. Depeursinge, *Biomed. Opt. Express* **2**, 2216 (2011).
- ¹⁴J. M. Coupland, R. Mandal, K. Polodhi, and R. K. Leach, *Appl. Opt.* **52**, 3662–3670 (2013).